Full Paper
Journal of Nano Materials Impact 2026, 02 (01) 29-34

Revealing The Influence of Substitutional Doping Nitrogen on Aluminum Phosphide Nanosheet: DFT Approach

Zahraa Ahmed Mohammed, Nibras Mossa Umran* Worood S. Rasool, M.A. Al-Kaabi
Department of Physics, College of Science, Kerbala University, Karbala 56001, IRAQ.

Abstract

This work investigates the electronic and optical properties of aluminium phosphide nanosheets (AlPNs) by examining the impact of varying nitrogen (N) atom concentrations, as dopants, via Density Functional Theory (DFT) calculations with the CASTEP code. Analysis of the electronic properties, band structure and density of states (DOS) revealed that the pristine AlPNs exhibit a band gap of 2.35 eV. The band gap showed a significant reduction to 1.79 eV upon doping with two N atoms, correlating directly with increased impurity concentration. Furthermore, the optical properties, including the absorption spectrum, reflectivity, and dielectric function, were calculated for both pristine and doped systems. The results indicate that controlled N doping can selectively enhance the optical activity within specific spectral ranges. These findings suggest that doped AlP nanosheets are promising materials for advanced optoelectronic devices and nanosensor applications.

Keyword: Doped AlPNs • DFT • CASTEP • Electronic and optical properties.

Introduction

Nanoscience and nanotechnology are witnessing a new era of fundamental research at the nanoscale, where the cost-effective fabrication of nano devices enables more robust scientific and engineering applications[1]. Recent advances in group III-V composite semiconductors have attracted considerable attention from the scientific community due to their promising potential in the electronics industry[2]. This impetus spurred a significant amount of theoretical and experimental research on group III-V semiconductor compounds, such as gallium phosphide (GaP), indium phosphide (InP), aluminum phosphide (AlP), and gallium arsenide (GaAs), etc. the Aluminum Phosphide (AlP) stands out as one of the most interesting materials due to its higher vibrational frequencies resulting from its low atomic mass[3], it's a semiconductor with a wide band gap of approximately 2.5 eV[3-7]. This bandgap enables its effective integration into various optoelectronic applications. Therefore, systematic computational studies form a pivotal stage that precedes and reinforces experimental characterization efforts for these nanostructures[8]. Observation of previous theoretical studies indicates that the zb-AlP nanocrystals, using the Ab initio restricted Hartree-Fock method coupled with the large unit cell method, determine that the cohesive energy and energy gap increase with the increasing size of the large unit cell for both core and surface parts[9-11].

***Address for correspondence:** Prof. Dr. Nibras Mossa Umran of Physics, College of Science, , Kerbala University, Karbala 56001, Iraq.

E-mail: nibrasmossa@uokerbala.edu.iq

ORCID: https://orcid.org/0000-0001-8916-2150

Info:
Submitted: 09 Dec. 2025; **Revised:** 26 Jan. 2026;
Accepted: 11 Feb. 2026; **Published:** 15 Feb. 2026.
https://doi.org/10.71109/nmi.2026.1.2.24

In this study, density functional theory (DFT) computations were employed to investigate the electronic and optical properties of pure Aluminum phosphide nanosheets[12]. To improve the material's performance and purposely vary its properties, the crystal structure was doped independently with nitrogen (Nn) where (n=1-3), doped and pure materials were carefully compared in terms of electronic properties, which include band gap width, as well as optical qualities, such as absorption coefficient. This research aims to offer essential insights into enhancing the functionality of AlP nanosheets and their modification for more efficient electronic and optical applications.

Theoretical Methods

All calculations in this work were performed using Density Functional Theory (DFT)[12], which is based on the plane-wave pseudopotential technique in the Cambridge Sequential Total Energy Package (CASTEP) codes[13]. The interaction between the ionic cores and valence electrons was modeled using the Ultrasoft pseudopotential. In the computation of structural, mechanical, and optical properties, we used the generalized gradient approximation (GGA) of the Perdew-Burke-Ernzerhof (PBE)[12]. It is acknowledged that the GGA-PBE functional might not be sufficient for quantitative analysis of optical qualities, but the estimated findings are also valuable for qualitative research and reference. A vacuum region larger than 15 Å (specifically 17.69Å) was introduced perpendicular to the nanosheet to prevent spurious interactions between periodic images caused by the periodic boundary condition. The kinetic energy cutoff for plane-wave expansion is set to 340 eV. For geometry optimization, a 5x5x1 k-point mesh was utilized, whereas a denser 9x9x1 grid was employed for electronic and optical property calculations. in the optical response, the number of empty bands was set to 100% of the occupied bands to ensure a sufficient energy range for electronic transitions. A Gaussian smearing of 0.1 eV was employed to obtain a well-resolved optical spectrum. The Broyden-Fletcher-Goldfarb-Shanno

(BFGS) algorithm was used for geometry optimizations[9], and the convergence tolerance parameters were taken as follows: a maximum stress of 0.1 GPa, a maximum residual force of 0.05eV/Å, a maximum displacement of 0.002Å, energy change of 2.0e-5 eV/atom. The above equation was used to calculate the binding energy (EB) to evaluate the system's stability[14], as follows:

$$E_B = [E_{tot}(M_nAlP) - (n_P * E_P + n_{Al} * E_{Al} + n_i * E_M)]/n \quad \text{... (1)}$$

Where E_B is the binding energy per atom. E_{tot} (MnAlP), E_P and E_{Al} are the total energies of the substitution doped Al_P and single Al, P and dopant atom of all elements, respectively. n_i is the number of i^{th} species present in the configuration and n is the total number of atoms in a supercell (n=50). The isolated atom energies were obtained from spin–polarized DFT calculations performed in large cubic boxes (15Å x15Å x 15Å) using the Ultrasoft pseudopotential and cutoff energy 340 eV to ensure minimal interactions between periodic images. While the vertical ionization potential (VIP) was calculated as the energy difference between the cationic and neutral Mn AlP complexes[15].

$$VIP = E_{(Cation)} - E_{(neutral)} \quad \text{... (2)}$$

Where VIP is referred to as Vertical ionization potential, E(cation), the total energy to complex one electron, E(neutral), the total energy of neutral AlP nanosheet. To obtain the cationic system, one electron was removed from the neutral supercell and a homogenous background charge was automatically introduced by CASTEP to neutralize the periodic cell. The calculated VIP was referenced to the vacuum level, determined from the planar- averaged electrostatic potential in the middle of the 17.69 Å vacuum spacing[16], ensuring comparability with experimental measurements.

Energy descriptors, including chemical potential (μ), chemical hardness (η), absolute chemical softness (S) and electrophilicity index (ω), were computed using HOMO and LUMO values. The following equations show the descriptors that were calculated[17, 18]:

$$\mu = -(-E_{HOMO} + E_{LUMO})/2 \quad \text{... (3)}$$

$$\eta = (-E_{HOMO} - E_{LUMO})/2 \quad \text{... (4)}$$

$$S = 1/\eta \quad \text{... (5)}$$

$$\omega = \mu^2/2\eta \quad \text{... (6)}$$

Results and Discussion

Structural and Stability

Optimize The Structure of N Doped AlP Nanosheets

The crystal structures of the two-dimensional AlP nanosheet and N doped AlP after full relaxation are shown in **Figure 1**. The initial model was constructed in a buckled hexagonal configuration using a 5x5x1 supercell to represent the isolated monolayer. Upon performing full geometry optimization, the system underwent structural refinement, transitioning from the initial buckled state into a stable planar hexagonal geometry, with a finalized monolayer thickness of 2.01Å. To ensure the accuracy of the electronic properties and eliminate any artificial interlayer coupling, a vacuum spacing of 17.69Å was maintained along the out-of-plane direction. Building on this stable hexagonal model, the AlP nanosheets structural response was assessed at different nitrogen (N) doping concentrations by methodically replacing the phosphorus (P) atoms in the nanosheet center. The hexagonal structure demonstrated exceptional integrity at a doping concentration of 2% (one N atom substitution), with an Al-N-Al angle of 120.0459° and an Al-N bond length stabilizing at 1.860 Å. The system successfully maintained its stable hexagonal form when the dopant density increased to 4% with two N atoms. This resulted in a slight contraction of the bond length to 1.8568Å. The observed instability is primarily due to a significant atomic size mismatch between the smaller N and larger phosphorus atoms, which causes localized compressive strain to accumulate within the supercells. While the hexagonal AlP lattice can withstand the strain caused by one or two dopants via bond relaxation, the third dopant exceeds the critical strain threshold, resulting in severe structural distortion and a lack of numerical convergence.

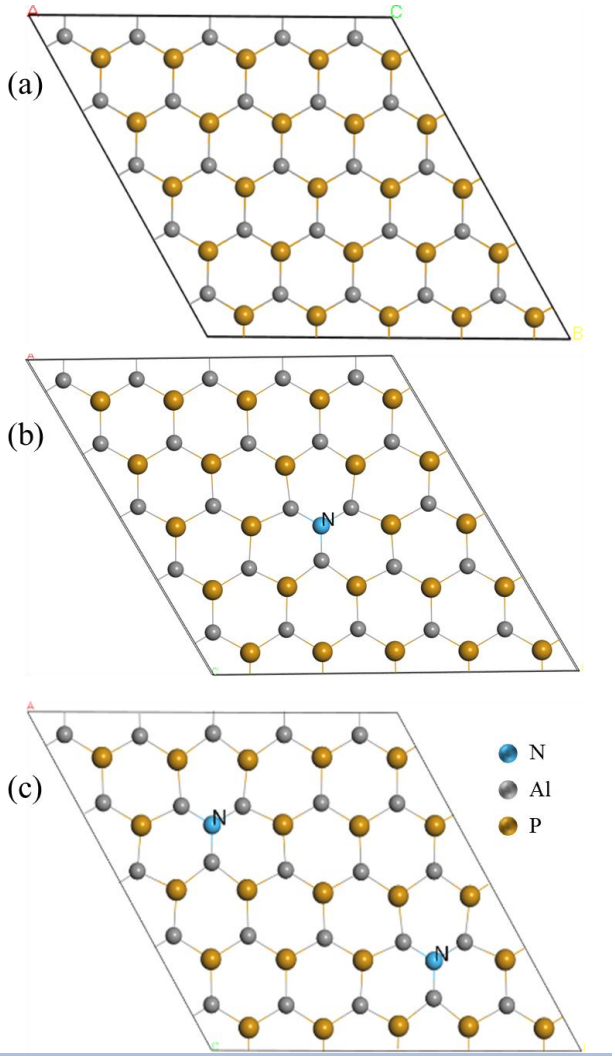

Figure 1. (a-c): The Optimized structure for AlP nanosheet, $N_1Al_{25}P_{24}$ and $N_2Al_{25}P_{23}$. the gray, orange and blue spheres refer to Al, P, and the dopant N atoms, respectively.

Furthermore, N high electronegativity causes excessive charge redistribution, which significantly increases the

formation energy and makes the triple-doped configuration thermodynamically unfavorable.

Binding Energy of N doped AlP Nanosheets

The binding energy of the doped systems has been determined to assess their stability for the optimized structures using equation (1). A negative binding energy indicates the presence of a metastable or stable bound dopant within the system. The binding energy (EB) value for pristine AlP nanosheet has been determined to be -4.51 eV/atom in good agreement with the value of -4.01 eV/atom[9]. The electronic properties observed in substitute doped AlP nanosheet with the number, position and type of dopant atoms and found that N atoms give rise to stable structure. **Table 1** shows the binding energy values of the element doped AlP nanosheet composites.

Table 1. Calculated Binding Energy (EB) for N doped AlP nanosheet.

Dopant AlP	E_B
$N_1Al_{25}P_{24}$	- 4.56 eV/atom
$N_2Al_{25}P_{23}$	-4.61 eV/atom

Electronic Properties

Band structure, Density of Sate (DOS) of Pure and N Doped AlP Nanosheets

To investigate the electronic band structures and DOS of pristine and doped AlPNs, as shown in **Figure2**. The results indicate that AlP has a direct bandgap, where the Valence Band Maximum (VBM) is dominated by the p -orbitals of the dopants, while the Conduction Band Minimum (CBM) shows significant hybridization between the Al-p and P-p states. Furthermore, doping it with N at varying concentrations was observed to cause a notable reduction in the Fermi level and progressive narrowing of the bandgap width.

Bandgap, Vertical Ionization Potential of Pure and N- Doped AlP Nanosheets

The impact of substitutional concentrations of 2% and 4% (one and two nitrogen atoms, respectively) of N doping on the electronic characteristics of AlP nanosheet was examined. The results reveal that the pristine material exhibits a direct bandgap of 2.35 eV. A gradual narrowing of the bandgap is observed with increasing doping concentration, reaching 1.82 eV upon doping with a single N atom (2%), and further decreasing to 1.79 eV when doped with 2N atoms (4%), as shown in **Table 2**. To evaluate the chemical stability and electronic activity of the nanosheets more deeply, global reactivity descriptors derived from density functional theory (DFT) were analyzed. The results showed that the chemical hardness (η) of the pristine compound was 1.177 eV, and it gradually decreased with increasing doping concentration, reaching 0.914 eV and 0.898 eV upon doping with (1N) and (2N), respectively. This decrease reflects the direct relationship between chemical hardness and bandgap. In contrast, the chemical softness (σ) values increased from 0.849 eV^{-1} for the pristine compound to 1.094 eV^{-1} and 1.113 eV^{-1} upon doping, clearly indicating an increase in the polarizability of the material and an enhancement of its chemical activity after the doping process. On the other hand, the electrophilicity index (ω) recorded a significant decrease from 0.782 eV for the pristine material to 0.290 eV at the highest doping concentration (2N). This sharp decrease indicates a reduction in the systems' ability to attract or accept electrons, reflecting a substantial change in the electronic nature of the material after doping. These results collectively indicate a clear shift in the thermodynamic stability and electronic properties of AlP nanosheets due to the introduction of new donor levels within the bandgap, enhancing their responsiveness to external stimuli- a promising feature for photocatalysis and sensor applications.

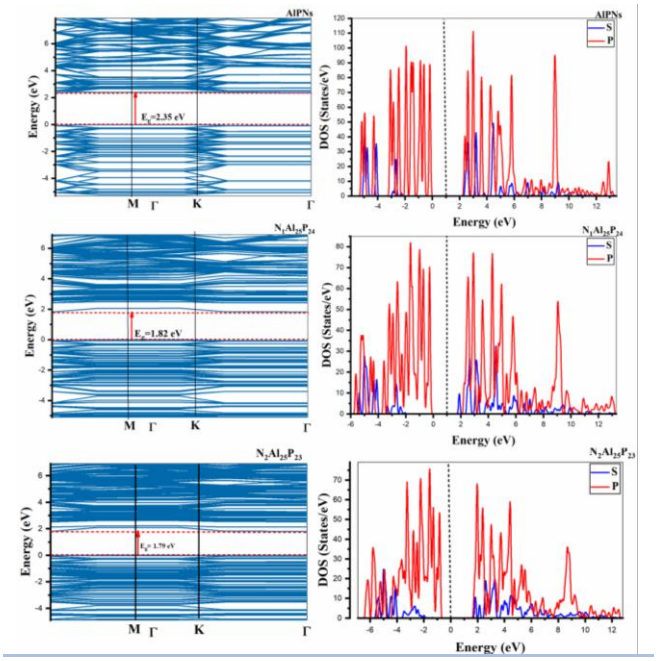

Figure 2. Band structure, DOS for AlP nanosheet, $N_1Al_{25}P_{24}$ and $N_2Al_{25}P_{23}$ respectively.

Table 2. Calculated Vertical Ionization Potential (VIP), Band gap, Chemical hardness (η in eV), Electrophilicity index (ω in eV) and Softness (S in eV^{-1}) for AlP, $N_1Al_{25}P_{24}$, $N_2Al_{25}P_{23}$.

Configurations	VIP (eV)	Bandgap (eV)	η (eV)	ω (eV)	S (eV^{-1})
AlP	2.67	2.35	1.177	0.782	0.849
$N_1Al_{25}P_{24}$	2.62eV	1.82	0.914	0.312	1.094
$N_2Al_{25}P_{23}$	2.58eV	1.79	0.898	0.290	1.113

Optical Properties of Pure and N-Doped AlP Nanosheets

The optical properties of a material can be described using the dielectric function, which can be expressed by the following relation[19-21]:

$$\varepsilon(\omega) = \varepsilon_1(\omega) + i\varepsilon_2(\omega) \quad \ldots (7)$$

The imaginary part of the dielectric function $\varepsilon_2(\omega)$ is a crucial factor in the study of 2D materials, as it represents the electronic transitions between occupied and unoccupied states and contains a wealth of information about the materials band structure[21]. Furthermore, many different optical spectra can be calculated based on it, other optical constants such as dielectric function, optical conductivity, absorption, reflectivity and refractive index were calculated. The optical properties of AlP nanosheets are significantly modified upon N doping Absorption spectra **Figure 3** reveal a distinct loe energy peak that red shift from ~1.8 eV for

single N atom doping to ~1.7 eV for double N atom doping. This red shift correlates with the calculated bandgap narrowing (from 2.35 eV to 1.79 eV), attributed to the introduction of in gap donor states. Concurrently, reflectivity exhibits notable broadening and shifts across the spectrum, resulting from doping induced lattice disorder and the redistribution of electronic states and optoelectronic applications.

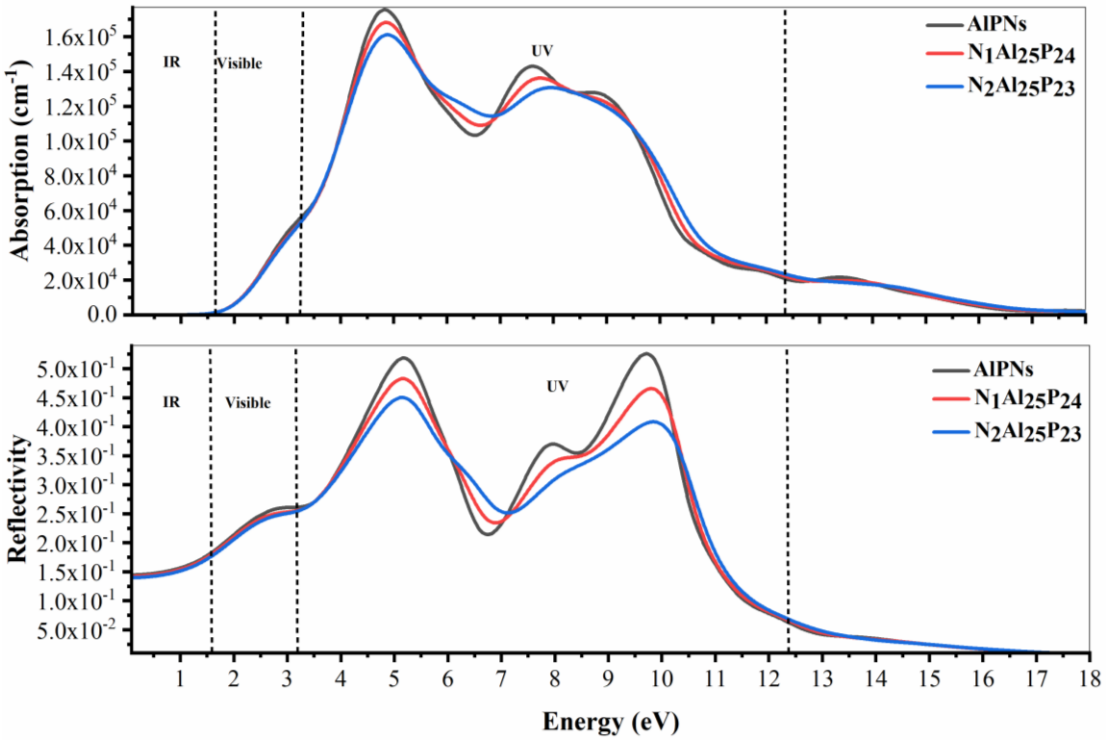

Figure 3. The Absorption and Reflectivity for AlP nanosheet, $N_1Al_{25}P_{24}$, and $N_2Al_{25}P_{23}$, respectively.

The dielectric function is depicted in **Figure 4** in relation to photon energy of the AlP nanosheet. In the real part (ε_1), doping with N causes a change in the dielectric response when compared to the pristine case, especially at lower energy levels, suggesting that the doped systems have improved electronic polarizability. The negative values of (ε_1) observed in the low energy region for doped systems indicate a highly reflective state, characteristic of semiconductor materials near their plasma frequency. This behavior arises from the collective oscillations of free carriers introduced by N doping.

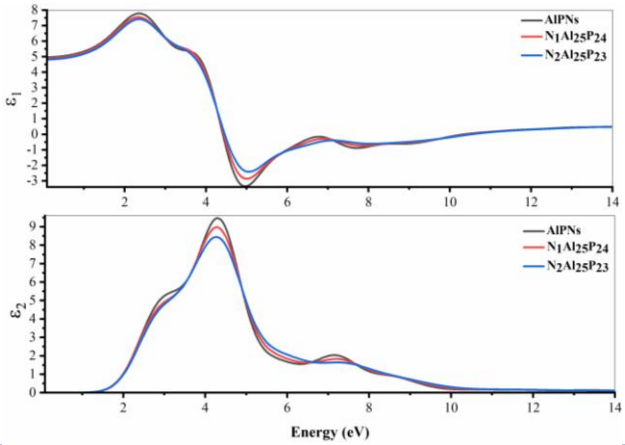

Figure 4. The calculated real part (ε_1) and imaginary part (ε_2) of the dielectric function for AlP nanosheet, $N_1Al_{25}P_{24}$, and $N_2Al_{25}P_{23}$, respectively.

The zero-crossing point of (ε_1), which defines the screened plasma frequency, shifts slightly upon doping due to increased carrier concentration, consistent with the enhanced reflectivity discussed (**Figure 5**). Regarding the imaginary part (ε_2), the results demonstrate a clear response for the doped configurations in the energy range 0f 1.5-3 eV, which represents optical absorption. New electronic transitions made possible by N-induced donor states within the bandgap are represented by these features along the energy axis. The distribution of the dielectric function confirms that doping the material with N improves its capacity to capture visible light.

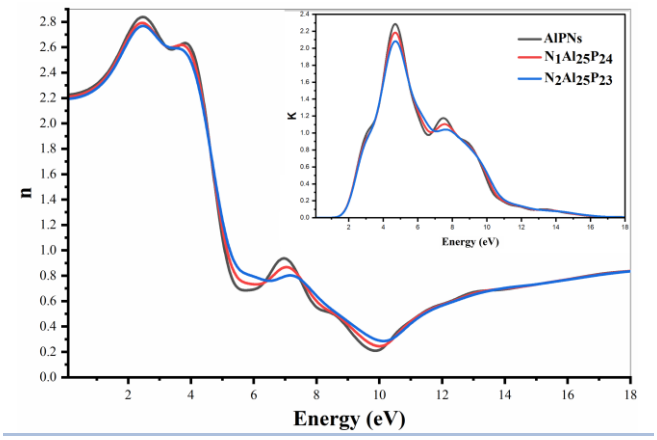

Figure 5. The calculated real part of the refractive index (n) and the extinction coefficient (k) for AlP nanosheet, $N_1Al_{25}P_{24}$, and $N_2Al_{25}P_{23}$, respectively.

gap states. This consistency between (n)and (k) confirms the successful modification of the material's optical behavior within the visible spectrum through doping.

To further evaluate the impact of the N- induced in gap states on charge carrier dynamics, the optical conductivity (σ) was investigated. As illustrated in **Figure 6**, the real part σ_1 exhibits significant conductivity peaks in the low energy region for the doped systems (N_1, N_2), whereas the pristine AlP nanosheet remains optically inactive in this range. This enhancement in optical conductivity aligns perfectly with the previously discussed extinction coefficient (k) and refractive index (n) results, confirming that N doping effectively triggers photo-induced electronic transitions within the visible spectrum. The increased conductivity for the double doped system (N_2) suggests a higher efficiency in light harvesting and charge generation, making these nanosheets highly suitable for visible light driven optoelectronic devices.

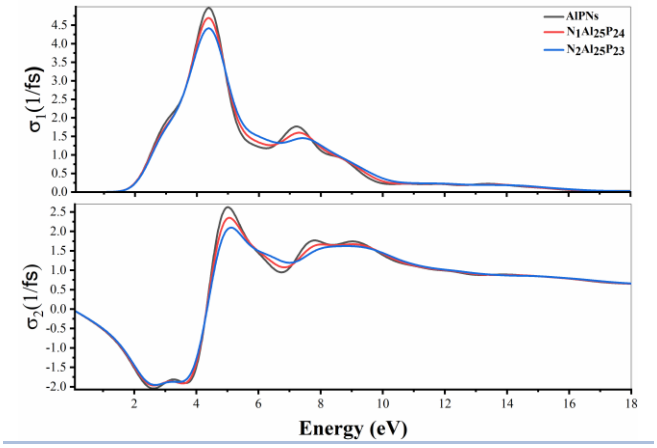

Figure 6. The calculated real part σ_1 and imaginary part σ_2 of the optical conductivity for AlP nanosheet, $N_1Al_{25}P_{24}$, and $N_2Al_{25}P_{23}$, respectively.

Conclusion

In summary, we systematically investigated the electronic and optical effects of N doping on monolayer AlP nanosheet using density functional theory (DFT)calculations. Binding energy calculations demonstrated that all studied conditions exhibited good thermal stability, indicating the potential for experimental fabrication of these doped nanosheets. The results revealed that the pure AlP possessed a band gap of 2.35 eV, while N doping led to a sharp decrease in the band gap with increasing concentration, while maintaining the semiconductor nature. Also, it has been calculated the optical properties, N doping significantly shifted the absorption edge towards lower energies, approximately 1.8 eV, thus broadening the optical response to include a portion of the visible spectrum. Ultimately, the results indicate that AlP-doped nanosheets hold promising potential for designing nano- optical devices with tunable properties.

Acknowledgements

The authors extend their sincere gratitude to the Castep group for making their computational code available. Furthermore, they wish to express their deep appreciation to the Department of Physics, College of Science, University of Kerbala, Karbala, Iraq, for their valuable scientific collaboration and support.

Funding

The authors declare that no external funding was received for this study.

Authorship Contribution

The authors contributed equally to the article.

Declaration of Competing Interests

The authors confirm that the publication of this paper is not impacted by any conflicts of interest.

References

[1] S. A. Saad and A. Elmahjubi, "Nanotechnology: Concepts, Importance and the Current State of Scientific Research," in *AIJR Proceedings*, 2018, pp. 552–562. https://doi.org/10.21467/proceedings.4.22.

[2] G. Li *et al.*, "Recent advances in III–V nitrides: properties, applications and perspectives," *Journal of Materials Chemistry C*, vol. 12, no. 32, p. 12150–12178, 2024. https://doi.org/10.1039/d4tc02615b.

[3] R. Chandiramouli, S. Rubalya Valantina, and V. Nagarajan, "Band structure engineering and transport properties of aluminium phosphide nanoribbon – A first-principles study," *Superlattices and Microstructures*, vol. 76, p. 135–148, 2014. https://doi.org/10.1016/j.spmi.2014.10.013.

[4] M. R. H. Mojumder, M. S. Islam, and J. Park, "Germanene/2D-AlP van der Waals heterostructure: Tunable structural and electronic properties," *AIP Advances*, vol. 11, no. 1, p. 015126, 2021. https://doi.org/10.1063/5.0023448.

[5] H. Cui *et al.*, "Bandgaps properties of III-phosphides (BP, AlP, GaP, InP) materials excited by ultrasonic," *Optik*, vol. 177, p. 58–63, 2019. https://doi.org/10.1016/j.ijleo.2018.09.146.

[6] V. Emberger, F. Hatami, W. Ted Masselink, and S. Peters, "AlP/GaP distributed Bragg reflectors," *Applied Physics Letters*, vol. 103, no. 3, p. 031101, 2013. https://doi.org/10.1063/1.4813748.

[7] S. F. Mohammed, S. M. A. Ridha, A. M. Ghaleb, Z. T. Ghaleb, Y. Benkrima, and M. A. Abdullah, "Determination of Band Structure and Compton profiles for Aluminum-Arsenide Using Density Functional Theory," *East European Journal of Physics*, no. 2, p. 132–137, 2023. https://doi.org/10.26565/2312-4334-2023-2-12.

[8] S. Yuvaraja, V. Khandelwal, X. Tang, and X. Li, "Wide bandgap semiconductor-based integrated circuits," *Chip*, vol. 2, no. 4, p. 100072, 2023. https://doi.org/10.1016/j.chip.2023.100072.

[9] C. Liu, M. Hu, K. Luo, D. Yu, Z. Zhao, and J. He, "Novel high-pressure phases of AlP from first

principles," *Journal of Applied Physics*, vol. 119, no. 18, p. 185101, 2016.
https://doi.org/10.1063/1.4948678.
[10] R. Yang, C. Zhu, Q. Wei, and D. Zhang, "First-principles study on phases of AlP," *Solid State Communications*, vol. 267, p. 23–28, 2017.
https://doi.org/10.1016/j.ssc.2017.09.008.
[11] Y. Su, H. Wang, S. Li, W. Sun, D. Li, and F. Peng, "Stable multifunctional aluminum phosphides at high pressures," *Physical Chemistry Chemical Physics*, vol. 25, no. 8, p. 6392–6396, 2023.
https://doi.org/10.1039/d2cp05289j.
[12] P. Hohenberg and W. Kohn, "Inhomogeneous Electron Gas," *Physical Review*, vol. 136, no. 3B, p. B864–B871, 1964.
https://doi.org/10.1103/PhysRev.136.B864.
[13] X. Yang *et al.*, "Two-dimensional aluminum phosphide semiconductor with tunable direct band gap for nanoelectric applications," *RSC Advances*, vol. 10, no. 42, p. 25170–25176, 2020.
https://doi.org/10.1039/d0ra04424e.
[14] N. M. Umran, H. A. Rashed, F. K. Mohamad Alosfur, and N. J. Ridha, "Effect of substitution (Al and P) atoms in ZnO nanosheet on structural and electronic properties," *Journal of Physics: Conference Series*, vol. 1032, no. 1, p. 012045, 2018.
https://doi.org/10.1088/1742-6596/1032/1/012045.
[15] J. A. Santana, J. T. Krogel, J. Kim, P. R. C. Kent, and F. A. Reboredo, "Structural stability and defect energetics of ZnO from diffusion quantum Monte Carlo," *The Journal of Chemical Physics*, vol. 142, no. 16, p. 164705, 2015.
https://doi.org/10.1063/1.4919242.
[16] M. V. Ivanov, D. Wang, D. Zhang, R. Rathore, and S. A. Reid, "Vertical vs. adiabatic ionization energies in solution and gas-phase: probing ionization-induced reorganization in conformationally-mobile bichromophoric actuators using photoelectron spectroscopy, electrochemistry and theory," *Physical Chemistry Chemical Physics*, vol. 20, no. 40, p. 25615–25622, 2018.
https://doi.org/10.1039/c8cp02936a.
[17] H. Elhaes and M. A. Ibrahim, "Investigating the electronic properties of graphene oxide functionalized with benzoic acid," *Scientific Reports*, vol. 15, no. 1, p. 38105, 2025.
https://doi.org/10.1038/s41598-025-22839-w.
[18] M. Heidari Nezhad Janjanpour, M. Vakili, S. Daneshmehr, K. Jalalierad, and F. Alipour, "Study of the Ionization Potential, Electron Affinity and HOMO-LUMO Gaps in the Smal Fullerene Nanostructures," (in en), *Chemical Review and Letters*, vol. 1, no. 2, p. 45–48, 2018.
https://doi.org/10.22034/crl.2018.85215.
[19] X. M. Duan, C. Stampfl, M. M. M. Bilek, and D. R. McKenzie, "Codoping of aluminum and gallium with nitrogen in ZnO: A comparative first-principles investigation," *Physical Review B*, vol. 79, no. 23, p. 235208, 2009.
https://doi.org/10.1103/PhysRevB.79.235208.
[20] C. Mao, H. Ni, L. Qian, Y. Hu, and H. Huang, "Aluminum Phosphide van der Waals Bilayers with Tunable Optoelectronic Properties under Biaxial Strain," *Crystals*, vol. 13, no. 4, p. 597
https://doi.org/10.3390/cryst13040597
[21] P. Bisht, "Electronic and Optical Properties of 2d Materials and Their Van Der Waals Heterostructures Using Density Functional Theory," MSc, Chemical and Materials Engineering, San Jose State University, 2023.
https://doi.org/10.31979/etd.qmwd-pp4p.